Article

Nanochannel Array Plastics with Tailored Surface Chemistry

Javid Rzayev, and Marc A. Hillmyer

J. Am. Chem. Soc., **2005**, 127 (38), 13373-13379• DOI: 10.1021/ja053731d • Publication Date (Web): 31 August 2005

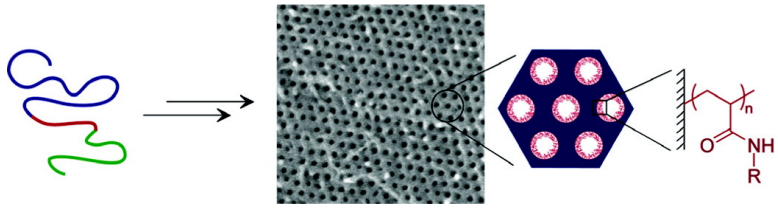

More About This Article

J|A|C|S
ARTICLES
Published on Web 08/31/2005

Nanochannel Array Plastics with Tailored Surface Chemistry

Javid Rzayev and Marc A. Hillmyer*

Contribution from the Department of Chemistry, University of Minnesota, Minneapolis, Minnesota 55455-0431

Received June 7, 2005; E-mail: hillmyer@chem.umn.edu

Abstract: The utilization of nanoporous substrates in applications such as selective ion transport, biomolecule separation, seeded templating, and catalysis necessitates the ability to efficiently control pore surface properties. We approached this task by preparing nanoporous polymer monoliths from ABC triblock copolymer precursors that assemble into a cylindrical morphology, where the A block constitutes matrix, C is the removable minor component, and B provides the functionality on the surface of the pores. Polystyrene−polydimethylacrylamide−polylactide (PS−PDMA−PLA) triblock copolymers were prepared by a combination of controlled ring-opening and free-radical polymerization techniques. After selective etching of the PLA cylinders from shear-aligned monoliths, a nanoporous polystyrene matrix containing a hexagonally packed array of hydrophilic, PDMA-coated channels was obtained. Extremely high degrees of alignment and order could be attained, and nanoporous substrates with second-order orientation factors of as high as 0.96 were prepared. PDMA brushes inside the pores were then hydrolyzed in a controlled fashion to introduce a desired number of carboxylic acid groups to the internal pore surface. Carbodiimide mediated couplings with amines were then used to confirm the accessibility of the interior acidic groups and to render materials with different functional content. This modular approach allows for the convenient preparation of functionalized nanoporous materials from a single block copolymer precursor.

Introduction

The great utility of nanoporous materials comes from the combination of spatial confinement and high surface area that they provide. Certain applications, such as templating, surface patterning, and size selective separations, merely take advantage of the nanometer length scale features in these materials.[1] On the other hand, a broad range of applications rely on the increased substrate−surface interactions in nanoporous media.[2] Specific and nonspecific adsorption to the surface, interfacial chemical processes, and columbic interactions are among the principal concepts underlying affinity based separations, solid-supported catalysis, and electrokinetic transport. Thus, surface properties, such as surface energy, charge density, and functional group composition, must be carefully regulated to take full advantage of the high surface area offered by nanoporous materials.

The synthesis of both inorganic and organic nanoporous structures can be accomplished by a variety of techniques,[3,4] providing a diverse set of substrates, each with its own strengths and limitations. Inorganic matrices offer rigid mesoporous frameworks with exceptional thermal and chemical stabilities, while organic materials provide more flexible, mechanically tunable substrates, potentially open to further functionalization and manipulation. Ordered organic nanoporous materials can be prepared by using diblock copolymer precursors, where the incompatibility of the two segments (blocks) in the copolymer leads to microphase separation to provide a nanostructured precursor.[3] The ordered domains are then aligned, and the minority phase is removed by chemical etching, UV irradiation, or thermal treatment to provide the desired porosity. A range of diblock copolymers can be utilized to attain desired mechanical and chemical properties, and the easy processability of the precursor allows for convenient manipulation of the shape and alignment characteristics of the nanoporous matrix. Extensive efforts have been devoted to the preparation of nanoporous thin films from block copolymer precursors for the use in, for example, high-density storage media.[5] Significant advances have been made in preparation, alignment, and subsequent use of

(1) Hulteen, J. C.; Martin, C. R. *J. Mater. Chem.* **1997**, *7*, 1075. Jirage, K. B.; Hulteen, J. C.; Martin, C. R. *Science* **1997**, *278*, 655. Johnson, B. J. S.; Wolf, J. H.; Zalusky, A. S.; Hillmyer, M. A. *Chem. Mater.* **2004**, *16*, 2909. Kim, D. H.; Jia, X.; Lin, Z.; Guarini, K. W.; Russell, T. P. *Adv. Mater.* **2004**, *16*, 702. Martin, C. R. *Science* **1994**, *266*, 1961. Lakshmi, B. B.; Patrissi, C. J.; Martin, C. R. *Chem. Mater.* **1997**, *9*, 2544. Pearson, D. H.; Tonucci, R. J. *Science* **1995**, *270*, 68.

(2) Gasparac, R.; Mitchell, D. T.; Martin, C. R. *Electrochim. Acta* **2004**, *49*, 847. Hulteen, J. C.; Jirage, K. B.; Martin, C. R. *J. Am. Chem. Soc.* **1998**, *120*, 6603. Lee, S. B.; Mitchell, D. T.; Trofin, L.; Nevanen, T. K.; Soederlund, H.; Martin, C. R. *Science* **2002**, *296*, 2198. Liu, J.; Fryxell, G. E.; Mattigod, S.; Zemanian, T. S.; Shin, Y.; Wang, L. Q. *Stud. Surf. Sci. Catal.* **2000**, *129*, 729. Nishizawa, M.; Menon, V. P.; Martin, C. R. *Science* **1995**, *268*, 700. Ying, J. Y. *AIChE J.* **2000**, *46*, 1902. Choi, M.; Kleitz, F.; Liu, D. N.; Lee, H. Y.; Ahn, W. S.; Ryoo, R. *J. Am. Chem. Soc.* **2005**, *127*, 1924.

(3) Hillmyer, M. A. *Adv. Polym. Sci.* **2005**, in press.

(4) Raman, N. K.; Anderson, M. T.; Brinker, C. J. *Chem. Mater.* **1996**, *8*, 1682. Schmid, G. *J. Mater. Chem.* **2002**, *12*, 1231. Pai, R. A.; Humayun, R.; Schulberg, M. T.; Sengupta, A.; Sun, J. N.; Watkins, J. J. *Science* **2004**, *303*, 507. Chan, V. Z. H.; Hoffman, J.; Lee, V. Y.; Iatrou, H.; Avgeropoulos, A.; Hadjichristidis, N.; Miller, R. D.; Thomas, E. L. *Science* **1999**, *286*, 1716. Zhao, D. Y.; Feng, J. L.; Huo, Q. S.; Melosh, N.; Fredrickson, G. H.; Chmelka, B. F.; Stucky, G. D. *Science* **1998**, *279*, 548. Hedrick, J. L.; Miller, R. D.; Hawker, C. J.; Carter, K. R.; Volksen, W.; Yoon, D. Y.; Trollsas, M. *Adv. Mater.* **1998**, *10*, 1049. Hatton, B.; Landskron, K.; Whitnall, W.; Perovic, D.; Ozin, G. A. *Acc. Chem. Res.* **2005**, *38*, 305. Hinds, B. J.; Chopra, N.; Rantell, T.; Andrews, R.; Gavalas, V.; Bachas, L. G. *Science* **2004**, *303*, 62.

these materials in surface patterning.[6] On the other hand, applications such as supported catalysis, confined crystallization, selective transport, and separations require macroscopic samples of well-aligned nanoporous substrates. Recently, Zalusky et al. reported a chemical etching procedure capable of generating nanoporous matrixes from monolithic pieces of a polystyrene−polylactide (PS−PLA) precursor.[7] Shear-aligned PS−PLA diblock copolymers exhibiting cylindrical morphology were subjected to basic hydrolysis/alcoholysis, which effectively removed PLA cylinders and provided nanoporous PS. A distinct but related etching protocol has also been developed for poly(ethylene oxide) (PEO) containing block copolymer monoliths.[8] As a result of using diblock copolymer precursors, these methodologies provide single component matrices, the bulk properties of which, for the most part, dictate both the interior and the exterior surface chemistries. Hydrolytic etching of PLA leaves accessible hydroxyl groups inside the pores; however, the density of these groups is too low (ca. 0.25 per 1 nm^2) to have a significant influence on the overall surface properties of the pore walls.[7] In an attempt to circumvent this limitation, Mao et al. reported a blending strategy, which utilized two diblock copolymers with the same major component (PS) and two different but miscible (PLA and PEO) minor segments.[9] After selective removal of PLA, a nanoporous polystyrene matrix with internal PEO coating was obtained.

One of the advantages offered by the block copolymer route to nanoporous materials is the opportunity of expanding this basic framework for the construction of more sophisticated structures.[10] With appropriate molecular design, the addition of one or more functional segments into a block copolymer precursor can be used to build progressively more advanced architectures leading to tailored nanoporous materials.[11] In a preliminary account, we described the use of a triblock copolymer precursor, polylactide−polydimethylacrylamide−polystyrene (PLA−PDMA−PS), for the preparation of nanoporous polystyrene monoliths with hydrophilic, PDMA coated nanochannels.[12] Incorporation of an additional functional segment into the precursor block copolymer structure allowed for independent control of the interior surface properties of the nanoporous matrix. In this contribution, we show the versatility of this approach (Scheme 1) and describe the generic utility of PLA−PDMA−PS triblock copolymers as precursors to highly

Scheme 1. Preparation of Functional Nanoporous Monoliths from Triblock Copolymer Precursors

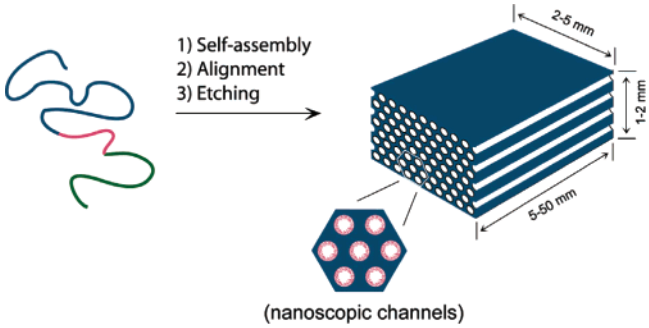

Scheme 2. Synthesis of PLA−PDMA−PS Triblock Copolymers

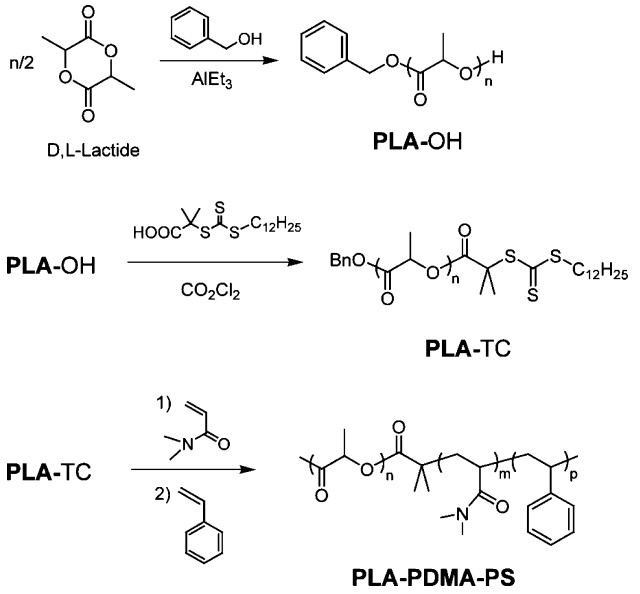

aligned, functionally diverse nanoporous materials, akin to nanochannel array glass reported over a decade ago.[13] The internal PDMA coating, stable under PLA etching conditions, was successfully hydrolyzed in a controlled fashion to install a desired number of carboxylic acid groups inside the pores, providing a convenient handle for further modifications. A variety of functional groups were incorporated into the nanoporous matrix using this modular approach. First, we report on the synthesis, morphological characterization, macroscale alignment, and selective etching of PLA−PDMA−PS triblock copolymer monoliths. We then describe a protocol for controlled chemical manipulation of the nanoporous substrates.

Results and Discussion

Polymer Synthesis. PLA−PDMA−PS triblock copolymers were synthesized by using a combination of controlled ring-opening and free-radical polymerization techniques (Scheme 2). The native hydroxyl end-group of PLA, prepared by aluminum catalyzed ring-opening polymerization of D,L-lactide, was coupled to the trithiocarbonate TC[14] via an acid chloride intermediate. As evidenced from NMR analysis, disappearance of the characteristic methine proton peak of the PLA end-group at 4.2 ppm and appearance of a new resonance with the same

(5) Mansky, P.; Harrison, C. K.; Chaikin, P. M.; Register, R. A.; Yao, N. *Appl. Phys. Lett.* **1996**, *68*, 2586. Thurn-Albrecht, T.; Steiner, R.; DeRouchey, J.; Stafford, C. M.; Huang, E.; Bal, M.; Tuominen, M.; Hawker, C. J.; Russell, T. P. *Adv. Mater.* **2000**, *12*, 787. Thurn-Albrecht, T.; Schotter, J.; Kastle, G. A.; Emley, N.; Shibauchi, T.; Krusin-Elbaum, L.; Guarini, K.; Black, C. T.; Tuominen, M. T.; Russell, T. P. *Science* **2000**, *290*, 2126.
(6) Shin, K.; Leach, K. A.; Goldbach, J. T.; Kim, D. H.; Jho, J. Y.; Tuominen, M.; Hawker, C. J.; Russell, T. P. *Nano Lett.* **2002**, *2*, 933. Mansky, P.; DeRouchey, J.; Russell, T. P.; Mays, J.; Pitsikalis, M.; Morkved, T.; Jaeger, H. *Macromolecules* **1998**, *31*, 4399. Olayo-Valles, R.; Lund, M. S.; Leighton, C.; Hillmyer, M. A. *J. Mater. Chem.* **2004**, *14*, 2729.
(7) Zalusky, A. S.; Olayo-Valles, R.; Taylor, C. J.; Hillmyer, M. A. *J. Am. Chem. Soc.* **2001**, *123*, 1519. Zalusky, A. S.; Olayo-Valles, R.; Wolf, J. H.; Hillmyer, M. A. *J. Am. Chem. Soc.* **2002**, *124*, 12761.
(8) Mao, H. M.; Hillmyer, M. A. *Macromolecules* **2005**, *38*, 4038.
(9) Mao, H. M.; Arrechea, P. L.; Bailey, T. S.; Johnson, B. J. S.; Hillmyer, M. A. *Faraday Discuss.* **2005**, *128*, 149.
(10) For examples of different morphologies observed in ABC triblock copolymers, see: Bates, F. S.; Fredrickson, G. H. *Physics Today* **1999**, *52*, 32. Epps, T. H., III; Cochran, E. W.; Bailey, T. S.; Waletzko, R. S.; Hardy, C. M.; Bates, F. S. *Macromolecules* **2004**, *37*, 8325. Breiner, U.; Krappe, U.; Abetz, V.; Stadler, R. *Macromol. Chem. Phys.* **1997**, *198*, 1051. Ott, H.; Abetz, V.; Altstaedt, V. *Macromolecules* **2001**, *34*, 2121. Stadler, R.; Auschra, C.; Beckmann, J.; Krappe, U.; Voight-Martin, I.; Leibler, L. Macromolecules **1995**, *28*, 3080.
(11) Liu, G.; Ding, J.; Stewart, S. *Angew. Chem., Int. Ed.* **1999**, *38*, 835.
(12) Rzayev, J.; Hillmyer, M. A. *Macromolecules* **2005**, *38*, 3.
(13) Tonucci, R. J.; Justus, B. L.; Campillo, A. J.; Ford, C. E. *Science* **1992**, *258*, 783.
(14) Lai, J. T.; Filla, D.; Shea, R. *Macromolecules* **2002**, *35*, 6754.

Table 1. Molecular and Structural Characteristics of PLA−PDMA−PS Triblock Copolymers[a]

triblock	$M_{n,PDMA}$[b]	$M_{n,PS}$[b]	$M_{n,total}$[b]	M_w/M_n[c]	f_{PLA}[d]	f_{PDMA}[d]	f_{PS}[d]	morphology[e]
1	2.2	42	55	1.19	0.17	0.04	0.79	Hex
2	6.6	40	58	1.14	0.17	0.10	0.73	Hex
3	3.2	29	43	1.12	0.23	0.07	0.71	Hex
4	11	45	67	1.19	0.15	0.15	0.70	Hex
5	2.2	25	38	1.14	0.26	0.05	0.69	Hex
6	2.3	22	35	1.12	0.28	0.06	0.66	Hex
7	6.7	27	45	1.17	0.22	0.14	0.64	L
8	2.2	20	33	1.13	0.30	0.06	0.64	L
9	11	29	51	1.18	0.19	0.20	0.61	L
10	18	31	60	1.24	0.17	0.27	0.56	L

[a] $M_{n,PLA}$ = 11 kg/mol (NMR analysis). [b]Molecular weights calculated from NMR analysis. [c]Obtained from SEC (PS standards). [d]Volume fractions calculated using known densities: $\rho_{PLA} = 1.25$,[17] $\rho_{PDMA} = 1.21$,[18] $\rho_{PS} = 1.04$[19] g/cm^3. [e]Morphologies as identified by SAXS at 25 °C after annealing at 160 °C for 15 min. L: lamellae. Hex: hexagonally packed cylinders.

relative intensity at 3.2 ppm, corresponding to the CH_2 next to the trithiocarbonate unit in PLA-TC, complete conversion was achieved. Trithiocarbonate end-capped PLA was subsequently used to consecutively grow PDMA and PS blocks by reversible addition−fragmentation chain transfer (RAFT) polymerization. High blocking efficiency was ascertained by size exclusion chromatography (SEC) for all steps, and final triblock copolymers were obtained with molecular weight distributions in the range 1.1−1.2. This protocol was used to prepare a range of PLA−PDMA−PS triblock copolymers with various compositions (Table 1). Given the functional group tolerance of free-radical polymerizations in general, and a versatility of the RAFT polymerization[15] in particular, this approach can be easily extended to the synthesis of other PLA containing block copolymers.[16]

Microphase Separation and Alignment. Powder samples of PLA−PDMA−PS triblock copolymers were pressed into a rectangular mold and then processed at 160 °C in a home-built channel die[7] to obtain macroscale oriented monolithic pieces (typical dimensions $W \times H \times L$: 2 × 2 × 5 mm^3). Small-angle X-ray scattering (SAXS) analysis was used to identify morphologies and alignment characteristics of the samples. Prior to channel die treatment, all pressed and annealed (190 °C, 20 h) triblocks showed a strong and narrow primary peak, consistent with microphase separation. For lamellae samples, two or three higher order reflections were also identified; however, for most of the other triblocks, secondary peaks appeared to be relatively broad and prevented unambiguous identification of the morphology. When these unidentified triblock samples were shear aligned in a channel die prior to annealing, SAXS patterns showed easily identifiable higher order reflections which confirmed the formation of a cylindrical morphology with hexagonal symmetry (Figure S1, Supporting Information). No order−order or order−disorder transitions (ODT) were observed by SAXS up to 180 °C in any sample. The desired cylindrical morphology was obtained only for samples with relatively high PS content ($f_{PS} \geq 0.66$, Table 1), where polystyrene presumably constitutes the matrix.

The degree of orientation in the monolithic pieces was calculated from 2D SAXS patterns using the normalized

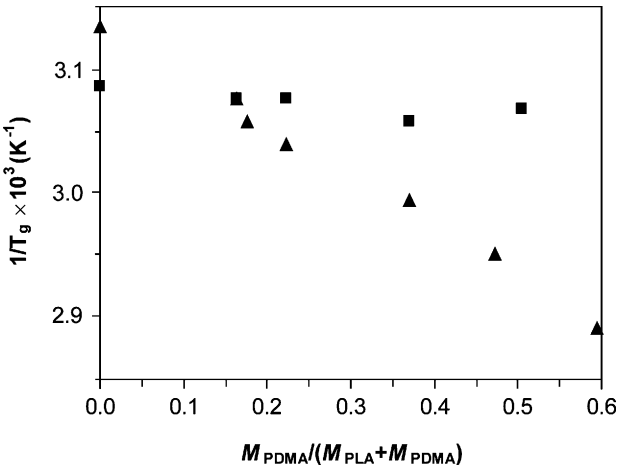

Figure 1. Dependence of the glass transition temperature of the PLA component on the weight fraction of PDMA in PLA−PDMA for PLA−PDMA diblock (triangles) and PLA−PDMA−PS triblock (squares) copolymers.

orientation distribution function $P(\phi)$ (eq 1).[7,20] Shear alignment of triblock copolymers using the channel die and subsequent annealing (190 °C, 20 h) proved to be very effective. In particular, for lower molecular weight samples **3**, **5**, and **6**, second-order orientation factor F_2 (eq 2) values of 0.92−0.96 were calculated. For other triblocks, less oriented samples were obtained ($F_2 \approx 0.8$). Annealing aligned monoliths seemed to slightly improve the degree of orientation.

$$\boldsymbol{P}(\phi) = \frac{I(q^*,\phi)q^{*2}}{\int_0^{\pi} I(q^*,\phi)q^{*2} \sin\phi \, \mathrm{d}\phi} \tag{1}$$

where q^* is the primary scattering vector, ϕ is the azimuthal angle, and $I(q^*,\phi)$ is the scattering intensity.

$$\boldsymbol{F}_2 = 1 - 3\langle\cos^2\phi\rangle \tag{2}$$

where

$$\langle\cos^2\phi\rangle = \int_0^{\pi} \cos^2\phi \, P(\phi) \sin\phi \, \mathrm{d}\phi.$$

Differential scanning calorimetry (DSC) was employed to help provide an insight into the arrangement of the blocks in the cylindrical morphology as identified by SAXS. First, parent PLA−PDMA diblock copolymers (Scheme 2) were investigated to establish the miscibility of these two segments. In the studied composition range, only one glass transition temperature (T_g) was observed, located between PLA (46 °C, M_n = 11 kg/mol) and PDMA (114 °C, M_n = 11 kg/mol) homopolymers. The transition temperature increased with PDMA content in the copolymer, with an inverse of T_g showing linear dependence on the weight fraction of PDMA (Figure 1), suggesting that PLA and PDMA are miscible in the investigated molecular weight and composition range. A drastically different behavior was observed in the case of PLA−PDMA−PS triblock copoly-

(15) Moad, G.; Rizzardo, E.; Thang, S. H. *Aust. J. Chem.* **2005**, *58*, 379.
(16) For other RAFT based approaches to PLA containing block copolymers, see: You, Y.; Hong, C.; Wang, W.; Lu, W.; Pan, C. *Macromolecules* **2004**, *37*, 9761. Hales, M.; Barner-Kowollik, C.; Davis, T. P.; Stenzel, M. H. *Langmuir* **2004**, *20*, 10809.
(17) Grijpma, D. W.; Penning, J. P.; Pennings, A. J. *Colloid Polym. Sci.* **1994**, *272*, 1068.
(18) Gundogan, N.; Okay, O.; Oppermann, W. *Macromol. Chem. Phys.* **2004**, *205*, 814.
(19) Quach, A.; Simha, R. *J. Appl. Phys.* **1971**, *42*, 4592.
(20) deGennes, P. G.; Prost, J. *The Physics of Liquid Crystals*; Oxford University Press: New York, 1993. Sakurai, S.; Aida, S.; Okamoto, S.; Ono, T.; Imaizumi, K.; Nomura, S. *Macromolecules* **2001**, *34*, 3672.

mers exhibiting the cylindrical morphology. For these samples, two glass transitions were identified, at 53 ± 1 °C and at 103 ± 1 °C, irrespective of the amount of PDMA in the copolymer (Figure 1). Both of the transition temperatures, which were attributed to the PLA and PS blocks, respectively, were virtually identical to those of a PLA−PS diblock copolymer with similar molecular weights.[21] The fact that PLA glass transition temperature is not affected by the amount of PDMA in the triblock implies the presence of a phase separated PLA domain, i.e., the addition of the third component (PS) into the copolymer forces PLA and PDMA to segregate. However, it is not clear whether all of the PLA exists in a phase separated domain; the possibility of formation of a broad interfacial region containing a partially mixed PLA−PDMA layer cannot be ruled out. Glass transitions corresponding either to the mixed PLA−PDMA layer or to the completely segregated PDMA block were not observed in any of the DSC traces, which could perhaps be attributed to the low weight fraction of the PDMA segment and the proximity of its transition to that of PS.

Interactions between different segments in a block copolymer are characterized by the Flory−Huggins parameter χ. Relative magnitudes of χ between any two blocks in a triblock copolymer have been shown to exert a strong influence on its morphology.[22] We performed a series of simple cross-comparison experiments to obtain a relative order of χ parameters for the PLA−PDMA−PS copolymer components. Knowing that PLA−PDMA diblocks do not phase separate over a broad range of compositions, while PS−PLA with similar molecular weights and PLA volume fractions have $T_{ODT} > 200$ °C,[7] we conclude that $\chi_{PS,PLA} > \chi_{PLA,PDMA}$. We also synthesized a PS−PDMA diblock copolymer by RAFT polymerization ($M_n = 12$ kg/mol, $M_w/M_n = 1.07$, $N_{tot} = 94$, $f_{PS} = 0.49$) and compared it to a PS−PLA diblock with similar compositional characteristics ($M_n = 12$ kg/mol, $M_w/M_n = 1.15$, $N_{tot} = 93$, $f_{PS} = 0.46$).[7] While the PS−PDMA copolymer was completely disordered, as confirmed by SAXS and DSC, its PS−PLA counterpart had a $T_{ODT} = 164$ °C, which implies that $\chi_{PS,PLA} > \chi_{PS,PDMA}$. These results indicate that the interaction between PS and PLA in the PLA−PDMA−PS system is the most unfavorable. The contact surface area between these two domains will, therefore, be minimized during the self-assembly process. In this scenario, it is reasonable to propose that PDMA acts to screen the energetically costly interactions between PS and PLA and, therefore, segregates to the interface between the PS matrix and PLA cylinders, leading to the formation of a core−shell cylindrical structure with PLA cores and PDMA (or possibly partially mixed PDMA−PLA) coronas.

Selective PLA Etching. Nanoporous monoliths were prepared by subjecting aligned PLA−PDMA−PS samples to basic hydrolysis conditions with a 0.5 M NaOH solution (MeOH/water = 40:60 v/v) at 65 °C. The rate of degradation was found to strongly depend on the size of the PDMA block. Thus, for samples with short PDMA chains (**3** and **5**) complete degradation was achieved within a few days, while for other triblocks

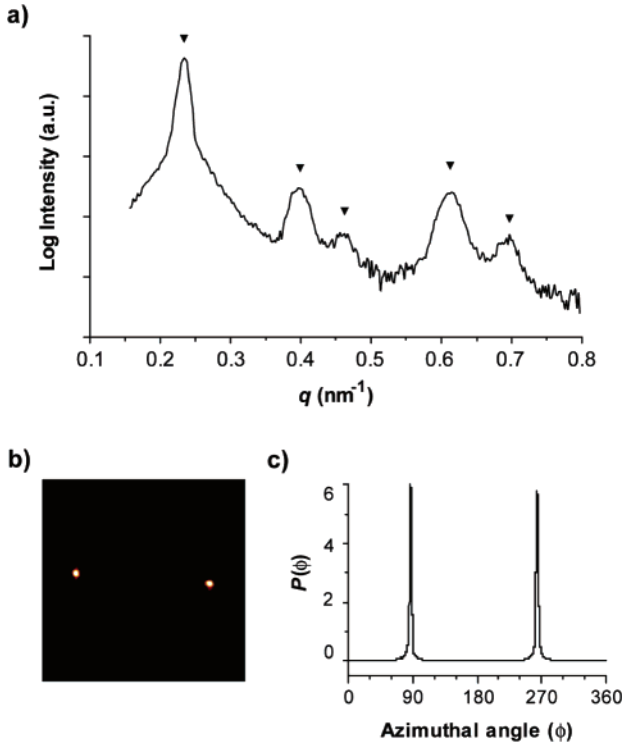

Figure 2. SAXS characterization of nanoporous PS−PDMA−**5** monoliths: (a) intensity vs scattering vector q (triangles indicate expected reflections for a hexagonally packed lattice, $1:\sqrt{3}:\sqrt{4}:\sqrt{7}:\sqrt{9}$), (b) 2D scattering profile, and (c) normalized orientation distribution function $P(\phi)$ vs azimuthal angle ϕ for the primary scattering peak ($F_2 = 0.96$).

(**2** and **4**) prolonged periods of 10−14 days were required to remove PLA entirely. The degradation at lower temperatures (25 °C) or in the absence of methanol proceeded successfully as well, albeit slower. NMR analysis confirmed complete removal of PLA and superb stability of the PDMA segment under these conditions. The process of etching PLA cylinders from the aligned monoliths depends on the interplay of several factors including the diffusion of the base into the pores, the rate of hydrolysis, and the diffusion of the reaction products (such as sodium lactide and oligolactide fragments) out of the pores. The fact that increasing the brush length inside the pores leads to substantially reduced degradation rates suggests a transport limited mode.

SAXS analysis of the degraded monoliths substantiated the formation of the nanoporous structure, which exhibited the same principal spacing and hexagonal symmetry as the precursor triblocks (Figure 2). Exceptional alignment was also preserved in the nanoporous monoliths, as evidenced by the calculated F_2 values as high as 0.96.[23] Scanning electron microscopy (SEM) provided real space images of the nanoporous structure. Figure 3 shows approximately 1 μm^2 area images of the nanoporous PS−PDMA monoliths fractured perpendicular and parallel to the pore alignment direction and clearly demonstrates the remarkable long range order that results from the channel die/annealing protocol. Pore sizes observed by SEM were in close agreement to those obtained from the SAXS analysis. A micrograph covering a larger area (ca. 42 μm^2) is included in

(21) The T_g at 52 °C, assigned to the PLA segment, was higher than that of the PLA homopolymer of the same molecular weight (46 °C), which could be attributed to one of the chain ends of PLA in the diblock being tied to the rigid PS matrix, or possibly to the nanoscopic confinement of PLA chains inside the PS.

(22) Bailey, T. S.; Pham, H. D.; Bates, F. S. *Macromolecules* **2001**, *34*, 6994. Bailey, T. S.; Hardy, C. M.; Epps, T. H.; Bates, F. S. *Macromolecules* **2002**, *35*, 7007.

(23) Due to the finite size of the beam, the highest obtainable F_2 value of 0.97 was estimated for the used SAXS instrument. The increase in calculated F_2 values in nanoporous monoliths compared to the undegraded samples is probably due to the enhanced signal-to-noise ratio.

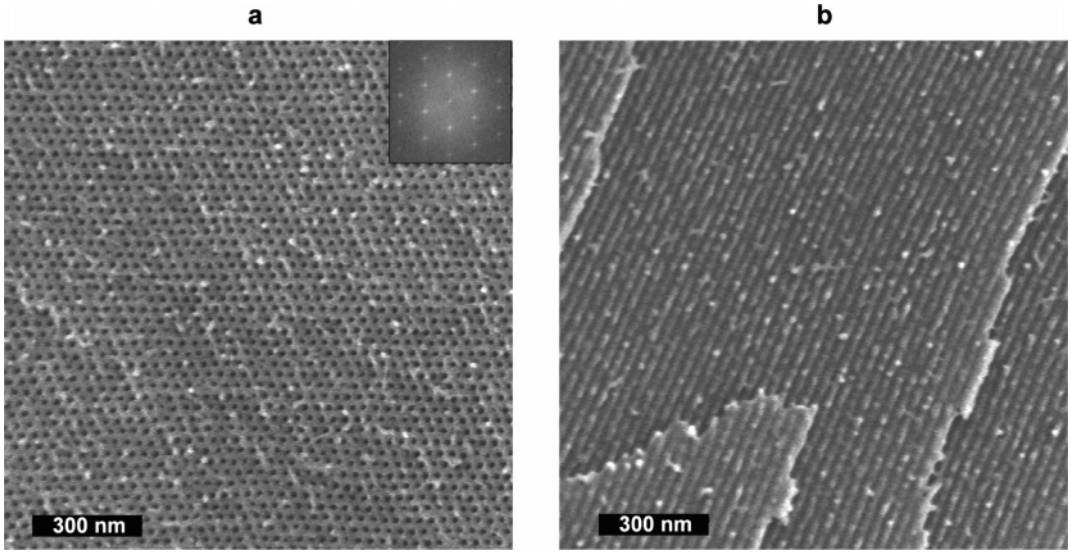

Figure 3. Scanning electron micrographs of nanoporous PS−PDMA−**5** monoliths fractured perpendicular (a) and parallel (b) to the pore alignment direction. The inset shows the result of Fourier transformation for the image (a).

Table 2. Structural Characteristics of Nanoporous Monoliths Prepared from PLA−PDMA−PS Triblock Copolymers[a]

precursor triblock	q^* (nm^{-1})	d_{pore}[b] (nm)	surface area (m^2/g)	t_{PDMA}[c] (nm)	F[d] (no./nm^2)
5	0.232	18.4	84	0.8	6
3	0.208	19.8	68	1.2	9
2	0.185	21.7	52	2.3	17
4	0.179	23.2	48	3.5	26

[a] All structural parameters were calculated using the primary scattering vector (q^*) of the nanoporous monoliths and volume fractions of the segments in the precursor triblock copolymer. [b]Pore diameter of the nanoporous polystyrene matrix. [c]Thickness of the PDMA layer inside the pores in the dry state. [d]Number of functional groups (dimethylamides) in units of the interior surface area.

Scheme 3. Hydrolysis of PDMA Chains Inside the Nanoporous PS−PDMA Monoliths

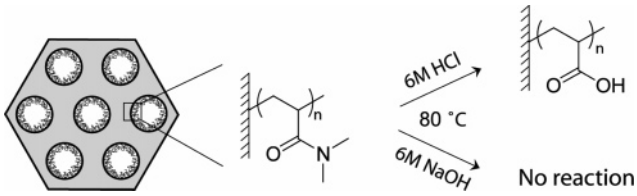

the Supporting Information material (Figure S2) as further evidence for the nearly defect-free, well ordered nanoporous structure. Fourier analysis of these images resulted in six spot patterns (see inset in Figure 3a), expected for a perfect hexagonally packed lattice, indicating the presence of large single grain domains over extended areas.

The thickness of the internal PDMA coating in nanoporous PS−PDMA monoliths could be regulated by choosing an appropriate triblock copolymer precursor. Table 2 shows structural characteristics of the nanoporous substrates prepared from different PLA−PDMA−PS triblocks containing identical PLA blocks and a progressively longer PDMA segment. The obtained materials possessed varying thicknesses of the PDMA coating, providing different densities of functional groups at the interior surface.

Hydrolysis of Internal PDMA Coating. The remarkable stability of PDMA under basic conditions was further verified by placing the samples of nanoporous PS−PDMA monoliths into a 6 M aqueous solution of NaOH. After 4 days at 80 °C, no signs of hydrolysis could be detected by NMR spectroscopy. On the other hand, when subjected to an acidic environment of 6 M HCl at 80 °C, the amide groups of PDMA hydrolyzed smoothly to provide carboxylic acid functionalities inside the pores (Scheme 3). After 2 days, complete conversion of PDMA to poly(acrylic acid) (PAA) was achieved under these conditions. Figure 4 shows IR spectra of PS−PDMA monoliths hydrolyzed for different periods of time. Peaks at 1645 and 1624 cm^{-1}, corresponding to the carbonyl stretch in PDMA (free and H-bonded, respectively), are progressively replaced by the peaks at 1729 and 1712 cm^{-1}, attributed to the carbonyl groups of PAA (free and H-bonded, respectively). Note that the predominant peaks in partially hydrolyzed monoliths are those of free PAA and H-bonded PDMA carbonyl groups, which is an indication of H-bonding formation between the amide and the carboxylic acid groups. In fact, PDMA and PAA are known to form intermolecular H-bonded aggregates in aqueous solutions due to the strong H-bond acceptor nature of the *N*,*N*-dimethylamide group.[24] Our mechanistic picture of the acid promoted

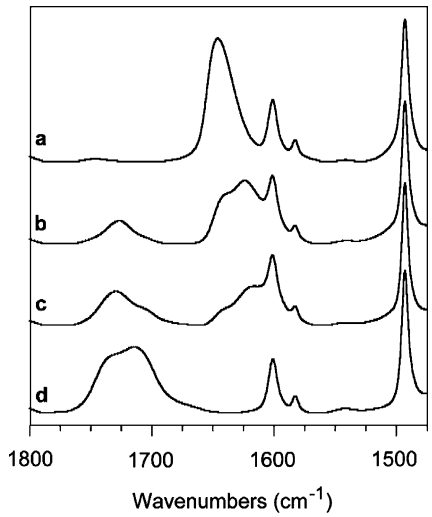

Figure 4. IR spectra of nanoporous PS−PDMA−**5** monoliths after acidic hydrolysis (6 M HCl, 80 °C) for (a) 0 h, (b) 5 h, (c) 10 h, and (d) 50 h.

Scheme 4. Functionalization of Nanoporous PS−PAA Monoliths Using EDAC Mediated Coupling with Amines

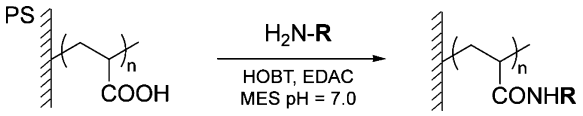

hydrolysis of PDMA brushes inside the pores is quite different from that of PLA degradation. At the beginning of the hydrolysis, the acid is present inside the pores in very high concentrations (6 M), which is higher (or comparable) to the concentration of amide groups in the pores depending on the specific sample used ($[amide]_0 \approx 2$ M for PS−PDMA−**5**). Therefore, the transport of the acid and end-products in and out of the pores becomes less significant in defining the overall reaction kinetics. Given the established resistance of amide groups toward hydrolysis in general and the fact that the surface PDMA layer is very thin, we propose that the slow rate of amide hydrolysis governs the overall rate of transformation.

Using the described protocol, nanoporous PS monoliths with internal PAA coating could be easily prepared. Remarkably, the nanoporous polystyrene matrix is stable under these harsh degradation conditions, as the retention of the structure was confirmed by SAXS (Figure S3). The utility of this two-step procedure, i.e., selective removal of PLA under basic conditions and subsequent hydrolysis of PDMA under acidic conditions, lies in its ability to easily modulate the density of carboxylic acid groups on the internal pore surface. By adjusting the hydrolysis time during the second step, nanoporous monoliths with a range of internal surface properties, from completely neutral and hydrophilic to highly charged, can be prepared starting from a single block copolymer precursor. On the other hand, if a maximum number of carboxylic acid groups is desired, the first step can be conveniently omitted as the acidic conditions alone will both degrade the PLA component and simultaneously hydrolyze PDMA brushes to directly provide PS−PAA monoliths.

Functionalization of Nanoporous Monoliths. The reactive PAA coating on the internal pore surface opens numerous opportunities for rendering the nanoporous matrix with diverse functional content. We have explored carbodiimide mediated coupling of amines and carboxylic acids as a surface modification strategy (Scheme 4). Reactions were conducted in an aqueous environment, with *N*-ethyl-*N*′-(3-dimethylaminopropyl)-carbodiimide (EDAC) as a reagent of choice due to its widespread use in protein modification chemistry.[25] The addition of 1-hydroxybenzotriazole (HOBT) greatly improved the yields, presumably by helping to turn over the EDAC adduct of carboxylic acids. The stability of EDAC in aqueous environment is known to be very dependent on the pH and chemical composition of the medium. While phosphate buffers have been widely used for EDAC mediated couplings before, it has been shown that the half-life of EDAC in the presence of phosphate reagents is greatly reduced.[26] We, therefore, carried out the functionalization of nanoporous monoliths in 2-morpholino-ethanesulfonic acid (MES) buffer at pH = 7.0, as these

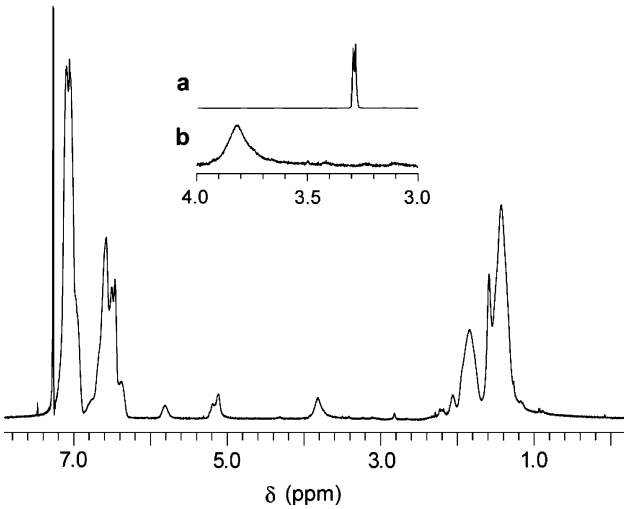

Figure 5. ^{1}H NMR spectrum ($CDCl_3$) of a nanoporous PS−PAA−**5** monolith modified with allylamine via an EDAC mediated coupling. The inset shows the expanded region for the allylic methylene peak in (a) initial allylamine and (b) allylamide of the modified monolith.

Scheme 5. Functional Nanoporous Materials Prepared from a Single PS−PAA Precursor.

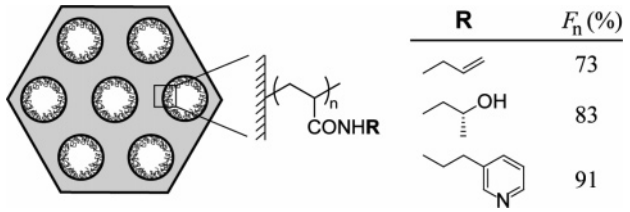

conditions have been identified to provide a much slower hydrolysis rate of EDAC, with $t_{1/2} \approx 20$ h.[26] Such a slow decomposition rate should provide enough time for EDAC to diffuse into the 5 mm long monoliths.

Chemical transformations were performed on nanoporous monoliths obtained from the triblock precursor **5**. The functional content of the modified substrates was characterized by NMR analysis. Figure 5 shows a ^{1}H NMR spectrum of a PS−PAA monolith reacted with allylamine under the described conditions. The resonances at 5.8, 5.1, and 3.8 ppm, corresponding to the *N*-allylamide group, present evidence for the successful attachment of the amine to PAA coated pore surface. Following this protocol, we were able to functionalize nanoporous PS−PAA monoliths with a variety of amines and incorporate different functional groups, such as a pyridine, a chiral hydroxyl, and an alkene, into the porous structure in good to excellent yields (Scheme 5). These results convincingly demonstrate accessibility and availability of the entire interior surface of the nanoporous monoliths for chemical manipulations.

Conclusions

We have demonstrated the synthesis of nanoporous polymer monoliths with tailored surface chemistry from block copolymer precursors. PLA−PDMA−PS triblock copolymers that self-assemble into a core−shell cylindrical structure have been identified, and their macroscale alignments have been employed to prepare highly oriented nanostructured materials. Protocols for the selective etching of PLA cylinders, controlled hydrolysis of PDMA fragments, and subsequent modification of the acidic groups on the pore surface have been developed. The robust

(24) Aoki, T.; Kawashima, M.; Katono, H.; Sanui, K.; Ogata, N.; Okano, T.; Sakurai, Y. *Macromolecules* **1994**, *27*, 947.
(25) Lundblad, R. L. *Chemical Reagents for Protein Modification*, 3rd ed.; CRC Press: Boca Raton, FL, 2005.
(26) Gilles, M. A.; Hudson, A. Q.; Borders, C. L. J. *Anal. Biochem.* **1990**, *184*, 244.

and versatile nature of the modification procedures allows for unprecedented control over the interior surface properties in mesoporous substrates. The methodologies for the synthesis and chemical manipulations of the nanoporous polymer monoliths elaborated in this work will provide an impetus for the utilization of these materials in a broad spectrum of applications, including selective transport and separations of biomolecules, water purification, supported catalysis, and confined crystallization.

Acknowledgment. The authors thank the National Science Foundation (DMR-0094144) and the David and Lucile Packard Foundation for financial support.

Supporting Information Available: Experimental details and Figures S1−S3. This material is available free of charge via the Internet at http://pubs.acs.org.

JA053731D